Cophosphorylation of amphiphysin I and dynamin I by Cdk5 regulates clathrin-mediated endocytosis of synaptic vesicles

Kazuhito Tomizawa,[1] Satoshi Sunada,[1] Yun-Fei Lu,[7] Yoshiya Oda,[4] Masahiro Kinuta,[2] Toshio Ohshima,[5] Taro Saito,[6] Fan-Yan Wei,[1] Masayuki Matsushita,[1] Sheng-Tian Li,[1] Kimiko Tsutsui,[3] Shin-ichi Hisanaga,[6] Katsuhiko Mikoshiba,[5] Kohji Takei,[2] and Hideki Matsui[1,7]

[1]Department of Physiology, [2]Department of Neuroscience, and [3]Department of Neuroanatomy, Okayama University
 Graduate School of Medicine and Dentistry, Okayama 700-8558, Japan
[4]Laboratory of Seeds Finding Technology, Eisai Co., Ltd., Ibaraki 300-2635, Japan
[5]Laboratory for Developmental Neurobiology, Brain Science Institute, RIKEN, Saitama 351-0198, Japan
[6]Department of Biological Sciences, Graduate School of Science, Tokyo Metropolitan University, Tokyo 192-0397, Japan
[7]Protein Therapy, New Techno-Venture Oriented R&D, Japan Science and Technology Corporation, Okayama 700-8558, Japan

It has been thought that clathrin-mediated endocytosis is regulated by phosphorylation and dephosphorylation of many endocytic proteins, including amphiphysin I and dynamin I. Here, we show that Cdk5/p35-dependent cophosphorylation of amphiphysin I and dynamin I plays a critical role in such processes. Cdk5 inhibitors enhanced the electric stimulation–induced endocytosis in hippocampal neurons, and the endocytosis was also enhanced in the neurons of p35-deficient mice. Cdk5 phosphorylated the proline-rich domain of both amphiphysin I and dynamin I in vitro and in vivo. Cdk5-dependent phosphorylation of amphiphysin I inhibited the association with β-adaptin. Furthermore, the phosphorylation of dynamin I blocked its binding to amphiphysin I. The phosphorylation of each protein reduced the copolymerization into a ring formation in a cell-free system. Moreover, the phosphorylation of both proteins completely disrupted the copolymerization into a ring formation. Finally, phosphorylation of both proteins was undetectable in p35-deficient mice.

Introduction

Clathrin-mediated endocytosis plays a key role in the recycling of synaptic vesicles in nerve terminals, and several components of the molecular machinery involved in this process have been identified as endocytic proteins (Cremona and De Camilli, 1997; Takei and Haucke, 2001). These include, in addition to clathrin, clathrin adaptors such as AP-2 and AP180, dynamin I, amphiphysin, synaptojanin I and endophilin (Cremona and De Camilli, 1997; Brodin et al., 2000). Endocytosis of the synaptic vesicles consists of four stepwise processes: nucleation, invagination, fission, and uncoating (Cousin and Robinson, 2001). Amphiphysin I and dynamin I play important roles in the invagination

and fission stages (Takei and Haucke, 2001). At the late invagination stage, amphiphysin I and dynamin I localize around the neck of the invaginated vesicles to form a collar (Takei et al., 1999; Cousin and Robinson, 2001). While the exact molecular mechanism by which fission is effected is not yet fully understood, it seems clear that hydrolysis of GTP by oligomeric rings of dynamin around the neck of endocytic intermediates is required for vesicle fission (Takei and Haucke, 2001).

The interactions among the various endocytic proteins are essential for the progression and maturation of clathrin-mediated endocytosis. For example, disruption of the amphiphysin I–dynamin I interaction results in the inhibition of synaptic vesicle endocytosis (Marks and McMahon,

The online version of this article includes supplemental material.

Address correspondence to Kazuhito Tomizawa, Department of Physiology, Okayama University Graduate School of Medicine and Dentistry, Shikata-cho 2-5-1, Okayama 700-8558, Japan. Tel.: 81-86-235-7109. Fax: 81-86-235-7111. email: tomikt@md.okayama-u.ac.jp
Key words: endocytic protein; p35; cyclin-dependent kinase; presynapse; synaptosome

1998). It has also been suggested that phosphorylation and dephosphorylation of the endocytic proteins regulate their interactions, resulting in the regulation of synaptic vesicle endocytosis (Marks and McMahon, 1998; Cousin and Robinson, 2001). Previous results showing that endocytic proteins undergo dephosphorylation during the maturation of clathrin-mediated endocytosis strongly support this suggestion (Bauerfeind et al., 1997; Slepnev et al., 1998). A Ca^{2+}/calmodulin-dependent phosphatase, calcineurin, plays an important role in the dephosphorylation (Slepnev et al., 1998). The switching from the phosphorylated state of the endocytic proteins to the dephosphorylated state after nerve terminal depolarization may trigger the clathrin-mediated endocytosis.

Cdk5 is a serine/threonine kinase with close structural homology to the cdc2 family (Dhavan and Tsai, 2001). Cdk5 forms a heterodimer with its neuron-specific activators, p35 or p39, and the association is essential for the kinase activation in neurons (Dhavan and Tsai, 2001). Cdk5 has multiple functions in neurons, implicating it in the regulation of a range of cellular processes from adhesion and motility to synaptic plasticity and drug addiction (Bibb et al., 2001; Dhavan and Tsai, 2001).

Cdk5 is abundant in presynaptic terminals in mature neurons (Tomizawa et al., 2002). Previous studies have identified many presynaptic proteins, such as Munc 18 (nSec-1) (Shuang et al., 1998), synapsin I (Matsubara et al., 1996), P/Q-type voltage-dependent calcium channel (Tomizawa et al., 2002), and amphiphysin I (Floyd et al., 2001), as substrates of Cdk5. These results suggest that Cdk5 is one of the most important kinases in the regulation of neurotransmitter release. Moreover, a very recent paper showed that Cdk5 phosphorylates dynamin I but not amphiphysin I, and the phosphorylation enhances synaptic vesicle endocytosis (Tan et al., 2003). However, this result is contradictory to the hypothesis of the trigger of synaptic vesicle endocytosis by calcineurin-mediated dephosphorylation of the endocytic proteins. Here, we show that Cdk5 phosphorylates both amphiphysin I and dynamin I in vitro and in vivo. The simultaneous phosphorylation of both these proteins inhibits synaptic vesicle endocytosis through inhibition of the association of these proteins with their partner proteins.

Results

Inhibition of Cdk5 activity enhances endocytosis in primary cultured neurons

To investigate whether Cdk5 regulates synaptic vesicle endocytosis, the fluorescent dye FM1-43 was used to stain the recycling vesicles in cultured hippocampal neurons. A stimulation of 20 Hz, 30 s was used to load the dye into the vesicle recycling pool by endocytosis (Pyle et al., 2000). Most of the loaded dye could be destained by an unloading stimulation. In control experiments, the first and second loading and unloading trials produced a similar fraction of active boutons (Fig. 1 A). After incubation with olomoucine (10 μM), a potent inhibitor of Cdk5, for 30 min, both the puncta number and size were increased. The total fluorescence (pixel size by average fluorescence intensity) increased to 290 $\pm$ 77% (Fig. 1 A; P < 0.005, compared

with the control group). Similarly, another Cdk5 inhibitor, roscovitine (10 μM), also produced an increase in the fluorescence (177 $\pm$ 31%, P < 0.05). On the other hand, an inactive analogue of olomoucine, iso-olomoucine (10 μM), did not produce any effects on FM1-43 dye uptake (92 $\pm$ 16%; Fig. 1 A).

The effect of 10 μM olomoucine was not likely to have been due to inhibition of MAP kinase, because the IC50 of olomoucine is 30–50 μM for MAP kinase (Vesely et al., 1994). To confirm this, U0126 (10 μM), a specific inhibitor of MAP kinase, was tested and found to have no effect on vesicle recycling (Fig. 1 A). These results suggest that Cdk5 plays a suppressive role in vesicle recycling.

The effect of olomoucine on vesicle exocytosis was also examined using a previously reported protocol with some modifications (Di Paolo et al., 2002). The rate of exocytosis was not affected by olomoucine when compared with the control group (Fig. 1 B). Thus, inhibition of Cdk5 seems to specifically enhance the endocytic process rather than the exocytic process.

The effects of inhibition of Cdk5 on the kinetics of vesicle endocytosis were then investigated. The vesicle recycling was initiated by depolarization, and FM1-43 was added after 30-, 60-, and 90-s delay times (Fig. 1 C, inset). Thus, only the vesicles that underwent endocytosis after the delay time were labeled, whereas those that underwent endocytosis during the delay period were not labeled. The active components of FM1-43 uptake at each delay time were normalized by that labeled at delay time 0 s (Fig. 1 C). When the delay time was longer, fewer endocytosed vesicles were stained. At each delay time point, the fraction of labeled vesicles was reduced by olomoucine treatment. These results suggest that more vesicles were endocytosed during the initial 30 s in the olomoucine-treated terminals. Thus, inhibition of Cdk5 increased the endocytic process.

In addition, the changes in total recycling pool size were also investigated. The total recycling pools were labeled by depolarizing the neurons with 90 mM KCl. Olomoucine increased the KCl-induced FM1-43 uptake (134 $\pm$ 6%, P < 0.05; Fig. 1 D). Taken together, these findings indicate that the inhibition of Cdk5 promoted the endocytic process and increased the total recycling pool size.

Vesicle endocytosis in p35-deficient mice

To further confirm the role of Cdk5 in endocytosis, the vesicle recycling in hippocampal neuronal cultures prepared from p35 knockout and wild-type embryonic mice was examined. Olomoucine increased the FM1-43 uptake in wild-type neurons (159 $\pm$ 10%; Fig. 1 E). In p35 knockout neurons, however, olomoucine did not produce any changes (96 $\pm$ 7%, P < 0.05, compared with p35 wild-type neurons). This result suggests that olomoucine enhanced the vesicle endocytic process by specific inhibition of Cdk5 activity.

The kinetics of vesicle endocytosis in p35 knockout neurons were also examined. The ratio of endocytosed vesicles after a 30–90-s delay time to that without a delay time in p35 knockout neurons was significantly reduced compared with that in p35 wild-type neurons (Fig. 1 F). This result is consistent with the changes in endocytic kinetics induced by olomoucine treatment in normal neuronal cultures (Fig. 1
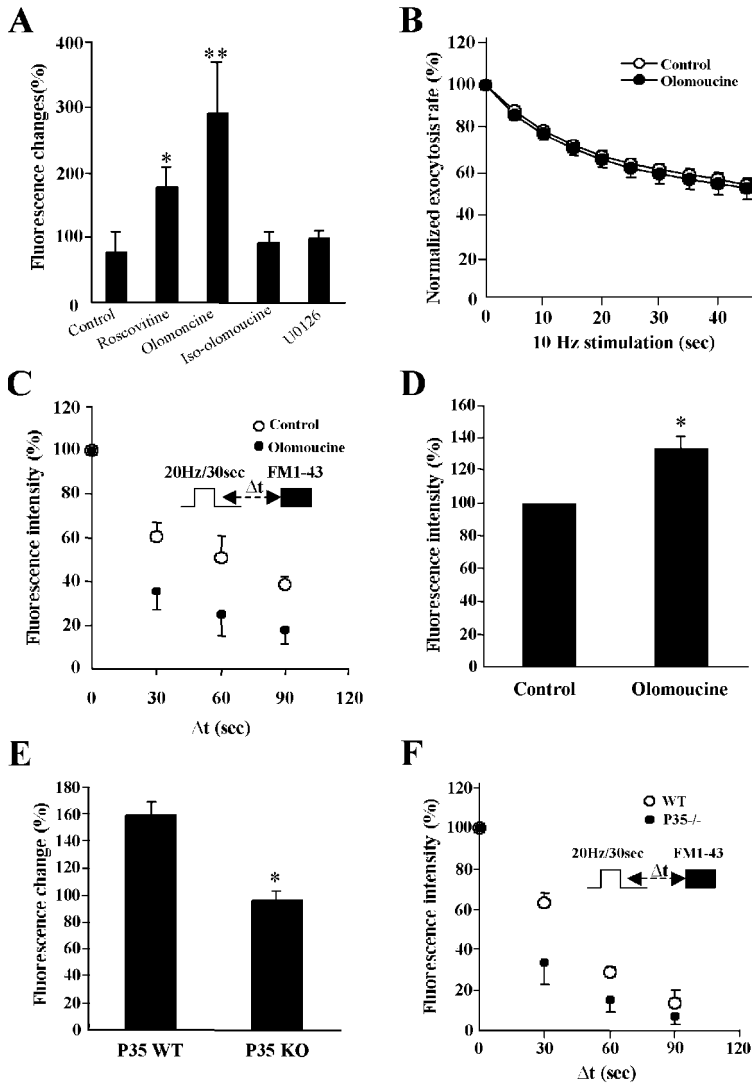
Figure 1. **Role of Cdk5 in vesicle endocytosis in hippocampal neurons.** (A) Summary of the effects of various agents on vesicle endocytosis. Data show the percentage changes in total fluorescence in the active boutons (total pixel size by mean fluorescence intensity) after drug treatment. Data express the mean $\pm$ SEM from five to eight experiments. *, P < 0.05; **, P < 0.005. (B) Effect of olomoucine on vesicle exocytosis. FM1-43 was loaded by a 20-Hz, 30-s stimulation. Olomoucine (10 μM) was added for 30 min. The vesicle exocytosis was then triggered by a 10-Hz, 45-s stimulation. During this period, sequential images were taken at 5-s intervals. The total fluorescence in the active boutons was measured and normalized by that immediately before exocytosis-triggering stimulation. (C) Effect of olomoucine on the kinetics of vesicle endocytosis. The inset shows the experimental protocol. A stimulus of 20 Hz, 30 s was delivered to depolarize the neurons. FM1-43 was then added after different delay times (Δt) and remained in the culture dish for 90 s. After washing with dye-free solution for 10 min, another 20-Hz, 30-s stimulus was delivered to unload FM1-43. The difference in FM1-43 fluorescence between loading and unloading was measured and normalized to that at Δt = 0. (D) Olomoucine-induced change in the total recycling vesicle size. The total recycling pool size was estimated by loading and unloading FM1-43 with 90 mM KCl. Data express the mean $\pm$ SEM from five experiments. *, P < 0.05. (E) Effect of olomoucine on vesicle recycling in p35-deficient mice. FM1-43 was loaded and unloaded by stimuli of 20 Hz, 30 s. Data show the changes in total fluorescence in the active boutons before and after olomoucine (10 μM, 30 min) treatment. Data express the mean $\pm$ SEM from three to five experiments. *, P < 0.05. (F) The kinetics of vesicle endocytosis in p35 knockout neurons. The inset shows the experimental protocol. A stimulus of 20 Hz, 30 s was delivered to depolarize the neurons. FM1-43 was loaded with a delay time of 30, 60, and 90 s. FM1-43 uptake at different delay time points was measured and normalized to that at Δt = 0.

C). Taken together, these findings reveal that Cdk5 plays an inhibitory role in vesicle endocytosis, and the suppression of endocytosis by Cdk5 is relieved in p35 knockout neurons.

Cdk5/p35 phosphorylates amphiphysin I and dynamin I in vitro

The specific substrates of Cdk5 in the synaptosomes were next identified. Solubilized synaptosomes from mouse brains were incubated with recombinant Cdk5/p35. Mass spectrometry showed the phosphorylation of both amphiphysin I and dynamin I from the synaptosomes (unpublished data). An in vitro kinase assay also revealed that both amphiphysin I and dynamin I were phosphorylated by Cdk5/p35 (Fig. 2 A). However, stoichiometric analysis showed that the number of phosphorylated residues differed between amphiphysin I and dynamin I. The maximum phosphate incorporation was 1.06 ± 0.03 mol of phosphate/mol of dynamin I (Fig. 2 B). Subsequent addition of fresh Cdk5/p35 at 60 min did not result in any further increase. In contrast, there were clearly multiple substrate sites suitable for Cdk5 in amphiphysin I. The maximum phosphate incorporation was 4.61 ± 0.1 mol of phosphate/mol of amphiphysin I (Fig. 2 B).

The phosphorylation sites of both the proteins were next determined by mass spectrometry. Most of the peaks of tryptic peptides of amphiphysin I in the spectra obtained by matrix assisted laser desorption/ionization mass spectrometry (MALDI-MS) could easily be assigned to the tryptic peptides predicted from the protein sequence. However, the biggest peak (260–292 residues, observed mass 3325.8 D) from unphosphorylated tryptic amphiphysin I (the arrowed peak in Fig. 3 A, top spectrum) disappeared upon phosphorylation, and six unassigned new peaks were observed in the MALDI-MS spectrum of phosphorylated amphiphysin (Fig. 3 A, middle spectrum). These peaks were candidate phosphorylated peptides because their observed masses were 80 D, or multiples of 80 D, higher than those calculated for the predicted tryptic peptides; for example, peak 1, 299–313 + P; peak 2, 260–292 + 2P; peak 3, 260–292 + 3P; peak 4, 260–298 + 3P; peak 5, 260–298 + 4P; and peak 6, 299–346 + P. These results suggest that Cdk5/p35 phosphorylates amphiphysin I at five sites in vitro. To determine the precise phosphorylation sites within the phosphorylated peptides, the remainder of the sample was subjected to liquid chromatography (LC)/MS/MS. The MS/MS spectrum of the doubly charged ion (m/z 818.8), which

Figure 2.   **In vitro phosphorylation of amphiphysin I and dynamin I by Cdk5.** (A) Autoradiography of Cdk5-dependent phosphorylation of amphiphysin I and dynamin I. Either recombinant amphiphysin I or purified dynamin I was incubated with/without recombinant Cdk5/p35 in the presence of γ-^{32}P [ATP] in vitro. (B) Stoichiometry of Cdk5-dependent phosphorylation of amphiphysin I and dynamin I. Amphiphysin I and dynamin I were phosphorylated with recombinant Cdk5/p35 for the indicated time periods. The amount of incorporated [γ-^{32}P]ATP was calculated after SDS-PAGE. (C) Migration shifts of phosphorylated wild-type amphiphysin I and the mutants by Cdk5/p35 on SDS-PAGE gel. After reaction with Cdk5/p35, the proteins were resolved by 6% SDS-PAGE and then immunoblotted with anti–amphiphysin I antibodies. Lanes 1 and 5, wild-type; lanes 2 and 6, serine 272, 276, and 285 residues to alanine; lanes 3 and 7, serine 261 and threonine 310 residues to alanine; lanes 4 and 8, all five residues to alanine. Lanes 1–4, dephospho-amphiphysin I; lanes 5–8, phospho-amphiphysin I. (D) Cdk5/p35-dependent incorporation of radiolabeled phosphate in wild-type and mutated recombinant amphiphysin I. Lane 1, wild-type; lane 2, serine 272, 276, and 285 residues to Ala mutant; lane 3, serine 261 and threonine 310 residues to Ala mutant; lane 4, all five residues to Ala mutant. (E) Phosphorylation of GST-PRD of wild-type dynamin I (WT) and threonine 780 to Ala mutant dynamin I (780 Ala). (F) Relative location of Cdk5-dependent phosphorylation sites in amphiphysin I and dynamin I. PH, pleckstrin homology domain.
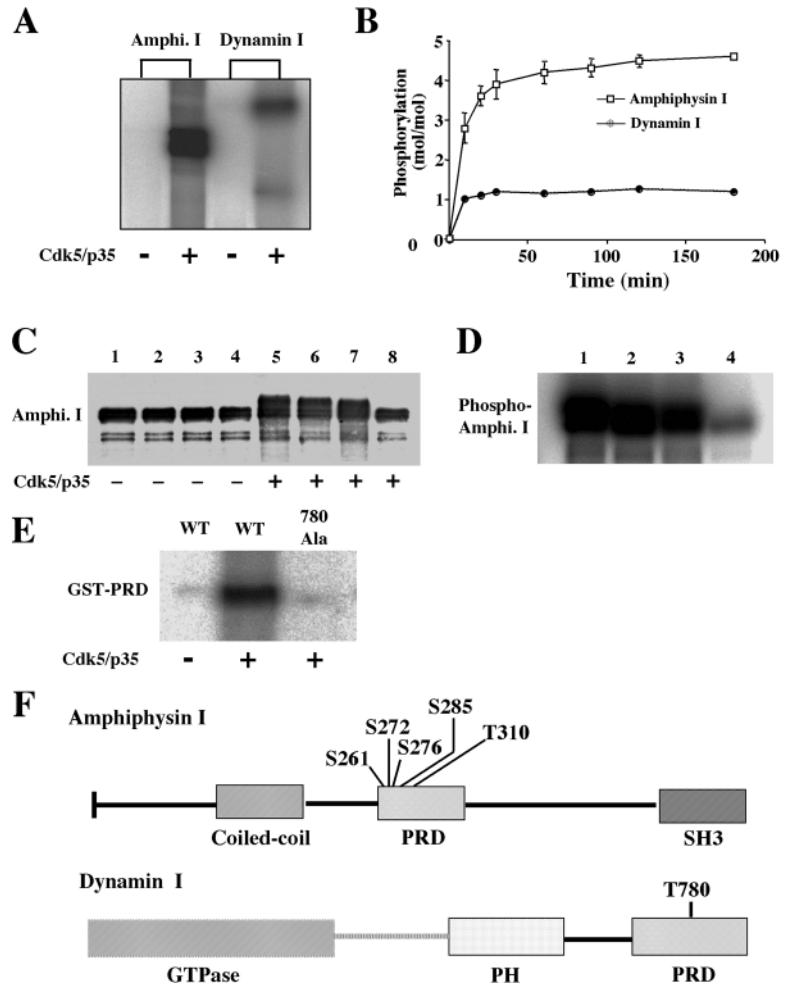
corresponded to peak 1 (299–313 + P) in MALDI-MS, is shown in Fig. 3 A, and on this basis, Thr310 was identified as a phosphorylation site (Fig. 3 A, bottom spectrum; this result also indicated that peak 6 had the same phosphorylation site at Thr310). However, other phosphorylated amino acids between residues 260 and 298 (peaks 2–4) were not assigned. To confirm the phosphorylation sites between amino acids 260 and 298 of amphiphysin I, serine/threonine sites in the region were mutated to alanine, and the phosphorylation of the mutant and wild-type proteins was compared. Wild-type amphiphysin I was phosphorylated by Cdk5/p35, and a mobility shift of the phosphorylated amphiphysin I in SDS-PAGE was observed (Fig. 2, C and D). A previous study showed that Cdk5 phosphorylates amphiphysin I at serine 272, 276, and 285 in vitro (Floyd et al., 2001). Therefore, a mutant of amphiphysin I in which these three sites were changed to Ala was prepared and subjected to the in vitro kinase reaction. Surprisingly, this mutant was still phosphorylated, and a mobility shift in SDS-PAGE was also observed (Fig. 2, C and D). Next, a similar mutant at serine 261 and threonine 310 was prepared and analyzed. This mutant was also phosphorylated (Fig. 2, C and D). However, Cdk5-dependent phosphorylation of a mutant in which all of these five sites were mutated to alanine was critically reduced, and no mobility shift in SDS-PAGE was observed (Fig. 2, C and D).

The phosphorylation site of dynamin I was next determined. MALDI-MS detected a phosphorylated peptide corresponding to 773–784 from the predicted tryptic peptides (unpublished data). However, this peptide included three SP or TP motifs (Fig. 3 B). To identify the precise phosphorylation site, LC/MS/MS analysis was performed and demonstrated that only Thr 780 of dynamin I was phosphorylated by Cdk5 (Fig. 3 B). To confirm the phosphorylation site of dynamin I, GST fusion protein of proline-rich domain (PRD) of wild-type and of threonine 780 to Ala mutant dynamin I was prepared and was subjected to the in vitro kinase reaction. The wild-type fusion protein was phosphorylated by Cdk5/p35 (Fig. 2 E). In contrast, Cdk5-dependent phosphorylation of the mutant fusion protein was markedly reduced, and the incorporation level of phosphate was the same as that in the absence of Cdk5/p35 (Fig. 2 E). These data agreed with that of the stoichiometric analysis shown in Fig. 2 B.

Effect of Cdk5-dependent phosphorylation of amphiphysin I and dynamin I on the interaction with those binding proteins

The present results showed that Cdk5/p35 phosphorylated the PRD of both amphiphysin I and dynamin I (Fig. 2 F). PRD of dynamin I interacts with the Src homology 3 (SH3) domain of amphiphysin I (Owen et al., 1998;
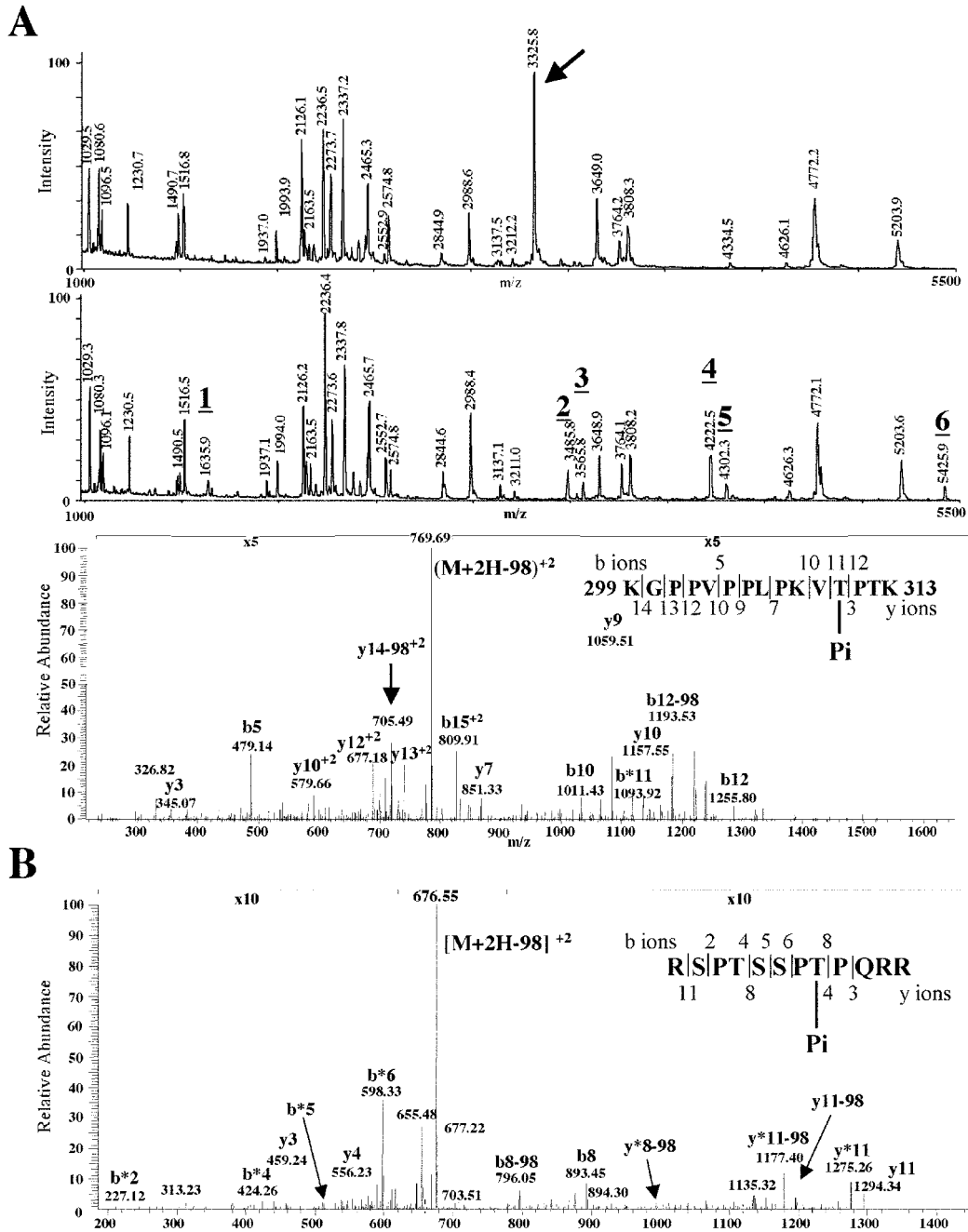
Figure 3. **Mass spectrometric analysis of amphiphysin I after in-gel tryptic digestion.** (A, top spectrum) MALDI-MS analysis of unphosphorylated amphiphysin I. The arrowed peak corresponds to residues 260–292. (A, middle) MALDI-MS analysis of phosphorylated amphiphysin I. Peak 1, 299 KGPPVPPLPKVTPTK 313 + 80 D; peak 2, 260 TPSPPEEPSPLPSPTA-SPNHTLAPASPAPARPR 292 + 160 D; peak 3, 260 TPSPPEEPSPLPSP-TASPNHTLAPASPAPARPR 292 + 240 D; peak 4, 260 TPSPPEEPSPL-PSPTASPNHTLAPASPAPARPRSPSQTR 298 + 240 D; peak 5, 260 TPSPPEEPSPLPSPTASPNHTLAPASPAPA-RPRSPSQTR 298 + 320 D; peak 6, 299 KGPPVPPLPKVTPTKELQ-QENIISFFEDNFVPEI-SVTTPSQNEVPEVK 346 + 80 D. (A, bottom) LC/MS/MS spectrum of doubly charged phosphorylated peptide (m/z 818.8, retention time 36.5 min) from tryptic peptides of phosphorylated amphiphysin I. (B) LC/MS/MS spectrum of a phosphorylated peptide of dynamin I after in-gel tryptic digestion.

Wigge and McMahon, 1998). On the other hand, PRD of amphiphysin I binds to the heavy chain of clathrin and the clathrin adaptor protein AP-2 (α- and β-adaptin; Wang et al., 1995; McMahon et al., 1997; Slepnev et al., 1998). Therefore, whether Cdk5-dependent phosphorylation of amphiphysin I and dynamin I affected the interaction with those binding proteins in vitro was examined. Phosphory-

lation of amphiphysin I by Cdk5 had no effect on the interaction with dynamin I (Fig. 4 A). However, the phosphorylation significantly inhibited its binding to β-adaptin (Fig. 4 B). Phosphorylation of dynamin I by Cdk5 inhibited the interaction with amphiphysin I (Fig. 4 C). As PRD of dynamin I interacts with the SH3 domain of amphiphysin I, the effect of the phosphorylation of dynamin I
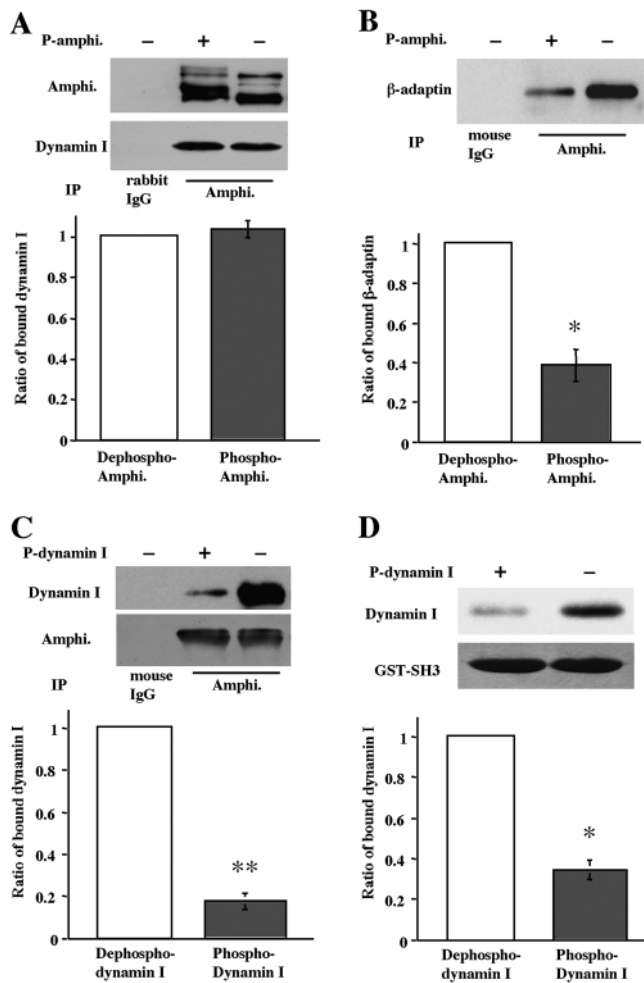
Figure 4. **Effect of Cdk5-dependent phosphorylation of amphiphysin I and dynamin I on the interaction with their partner proteins.** Quantitative analysis was performed as described in the Materials and methods. Bars, which have been normalized to the dephospho-amphiphysin I or dephospho-dynamin I (level of dephosphorylated form = 1), represent the mean $\pm$ SEM of four independent experiments. Statistical significance was calculated by the t test (*, P < 0.005; **, P < 0.001). (A) Interaction of phospho-amphiphysin I with dynamin I. Phospho- (5 μg) and dephospho-amphiphysin I (5 μg) were each incubated with purified dynamin I (4 μg). After immunoprecipitation with anti–amphiphysin I antibodies or rabbit Ig G, the complexes were subjected to Western blotting analysis with anti–dynamin I antibodies and anti–amphiphysin I antibodies. (B) Phosphorylation of amphiphysin I inhibited the interaction with β-adaptin. Phospho- and dephospho-amphiphysin I were incubated with rat brain lysates. Anti–amphiphysin I antibodies and protein G–Sepharose were then added for immunoprecipitation. The complexes were subjected to Western blotting analysis using anti–β-adaptin antibodies. (C) Interaction of phospho-dynamin I with amphiphysin I. Either phospho- or dephospho-dynamin I was incubated with purified dephospho-amphiphysin I. The amphiphysin I complexes were immunoprecipitated with the specific antibodies and then subjected to Western blotting analysis using anti–dynamin I antibody and anti–amphiphysin I antibody. (D) Effect of phospho-dynamin I on the interaction with the GST-SH3 domain of amphiphysin I. The GST-tagged SH3 domain of amphiphysin I was bound to glutathione–Sepharose beads, and phospho- or dephospho-dynamin I was then incubated with the beads. After the beads were washed, the complexes were subjected to Western blotting analysis with anti–dynamin I antibodies. Bottom panel, GST-SH3 polypeptides visualized by Coomassie blue staining of SDS-PAGE gel.

on the binding to the GST-SH3 domain of amphiphysin I was examined. The phosphorylation reduced the ability to interact with the GST-SH3 domain (Fig. 4 D). These results suggest that Cdk5-dependent phosphorylation of dynamin I and amphiphysin I regulates the interaction with their partner proteins.

Cdk5-dependent phosphorylation of both amphiphysin I and dynamin I disrupts the vesicle formation from liposomes

Previous studies suggested that amphiphysin I acts as a regulated linker protein that couples clathrin-mediated budding of endocytotic vesicles to dynamin-mediated vesicle fission (David et al., 1996; Takei et al., 1999). This phenomenon can be reconstituted as vesicle formation by dynamin I and amphiphysin I in a cell-free system (Takei et al., 1999). Upon the incubation of liposomes with dynamin I and amphiphysin I, liposomes project lipid tubules coated with these proteins, which are fragmented to generate small vesicles upon the addition of GTP (Takei et al., 1999). Furthermore, vesicle formation from liposomes can be assessed both qualitatively and quantitatively using dynamic light scattering (DLS) (Kinuta et al., 2002). Using these experimental systems, the effects of phosphorylation of dynamin I and amphiphysin I on vesicle formation were examined. Massive formation of small vesicles from the liposomes was induced by dynamin I and amphiphysin I in their dephosphorylated forms, but not in their phosphorylated forms, as observed by EM (Fig. 5 A). As revealed by DLS assay, the prepared unilamellar liposomes were >200 nm in average diameter, and no small vesicles were detectable (Fig. 5 B, a and f). After incubation of the liposomes with dephosphorylated dynamin I, dephosphorylated amphiphysin I, and GTP, a distinct peak of small vesicles (135.1 $\pm$ 21.8 nm in average diameter), which represented >76% of the total lipid vesicles in number, was detected by DLS (Fig. 5 B, b and f). Incubation of the liposomes with a combination of dephosphorylated dynamin I and phosphorylated amphiphysin I, or a combination of phosphorylated dynamin I and dephosphorylated amphiphysin I, also resulted in slightly less small vesicle formation (56.3 or 37.2% of the total lipid vesicles, respectively) (Fig. 5 B, c, d, and f). The small vesicle formation was almost completely abolished when the liposomes were incubated with the phosphorylated forms of both dynamin I and amphiphysin I (Fig. 5 B, e and f). These results suggest that Cdk5-dependent phosphorylation of both amphiphysin I and dynamin I regulates the coupling of clathrin-mediated budding of endocytotic vesicles to dynamin-mediated vesicle fission.

Effect of the Cdk5-dependent phosphorylation of dynamin I and amphiphysin I on the copolymerization into rings

Both amphiphysin I and dynamin I have an intrinsic property whereby they coassemble into rings without GTP and liposomes when admixed in a buffer of physiological ionic strength and pH (Takei et al., 1999). In agreement with previous studies, it was found that dynamin I forms only a very few rings under conditions of physiological ionic strength,
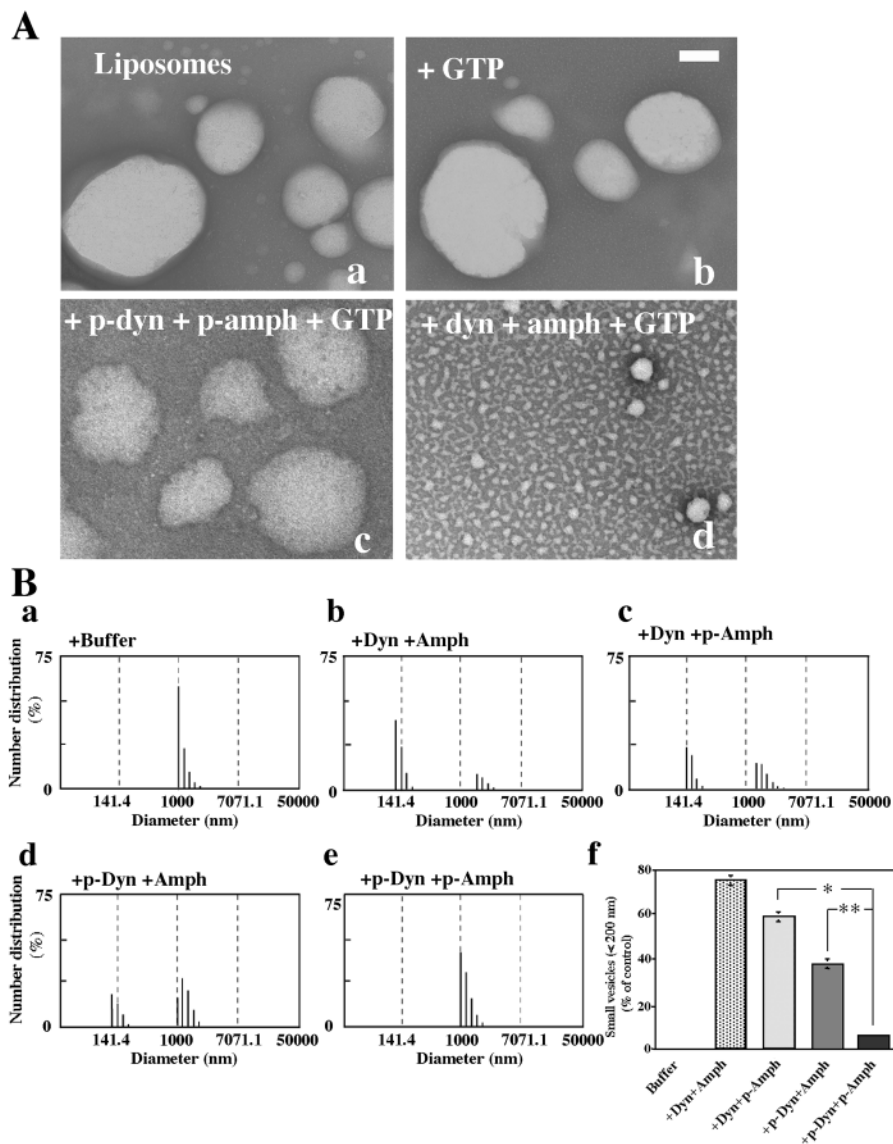
Figure 5. **Effect of phosphorylation of dynamin 1 and amphiphysin 1 on vesicle formation.** (A) EM observation of small vesicle formation from liposomes. Large unilamellar liposomes without incubation (a) or incubated under the indicated conditions (b–d) were negatively stained. The liposomes were almost unchanged after incubation with GTP only (b). Liposomes incubated with phosphorylated dynamin and phosphorylated amphiphysin were slightly deformed, probably because of bound proteins, but no small vesicles were formed (c). Massive formation of small vesicles was observed when liposomes were incubated with dephosphorylated dynamin 1 and dephosphorylated amphiphysin 1 (d). Bar, 200 nm. (B) Representative DLS assay of liposomes after incubation under the indicated conditions. The relative ratio of numbers of liposomes and lipid vesicles of each size were measured. (a) Control. Distinct peaks of small vesicles were evident when liposomes were incubated with dephosphorylated dynamin I and dephosphorylated amphiphysin I (b). The peaks of small vesicles were lowered when either of the proteins was phosphorylated (c and d). Almost no vesicle formation was observed when both dynamin and amphiphysin were phosphorylated (e). (f) Comparison of small vesicle formation under each condition shown in a–e. The relative numbers of small vesicles formed (<200 nm in diameter) from four independent experiments were averaged and graphed. Data are given as mean (±SEM). *, $P < 0.001$; **, $P < 0.005$ (by the Scheffe's test following two-way ANOVA).

while amphiphysin I alone never forms rings under these conditions (Fig. 6 A, a and b, and Fig. 6 B; Takei et al., 1999). However, massive and numerous rings were formed by a mixture of dephospho-amphiphysin I and dephospho-dynamin I ($80 \pm 11.2/\mu m^2$; Fig. 6 A, c, and Fig. 6 B). To demonstrate the effect of Cdk5-dependent phosphorylation of these proteins on ring formation, phospho-amphiphysin I and phospho-dynamin I were mixed, and the negatively stained proteins were observed by EM. The number of massive rings in the mixture of phospho-amphiphysin I and -dynamin I was markedly less than that in the mixture of the two dephosphorylated proteins ($18 \pm 7.2/\mu m^2$; Fig. 6 A, d, and Fig. 6 B). These results indicate that dephospho-amphiphysin I and -dynamin I can coassemble into ring structures, and Cdk5-dependent phosphorylation of these proteins inhibits the ring formations.

Comparison of the phosphorylation of amphiphysin I and dynamin I between wild-type and p35-deficient mice

To examine whether dynamin I is phosphorylated by Cd5/p35 in brain slices and synaptosomes, a phosphospecific polyclonal antibody for dynamin I that recognized phospho-dynamin I at Thr 780 was produced. The antibody recognized Cdk5-dependent phospho-dynamin I, but did not detect dephospho-dynamin I (Fig. 7 A). Previous studies have shown that FK506, a potent calcineurin inhibitor, prevents the lower mobility shift of amphiphysin induced by stimulated dephosphorylation (Bauerfeind et al., 1997; Slepnev et al., 1998). If Cdk5/p35 phosphorylated amphiphysin I in presynaptic terminals, the FK506-dependent mobility shift would be expected to be reduced in p35-deficient mice. A slight, but reproducible, electrophoretic mobility shift of amphiphysin I was consistently observed in the wild-type mouse synaptosomes in the presence of FK506, whereas no mobility shift was observed in the presence of a high concentration of K^+ (Fig. 7 B). In contrast, incubation of the synaptosomes from p35-deficient mice with FK506 failed to induce a mobility shift of the protein (Fig. 7 B).

Phospho-dynamin I–specific antibodies revealed that phospho-dynamin I was expressed in the synaptosomes from wild-type brain in the absence of FK506, and the phosphory-
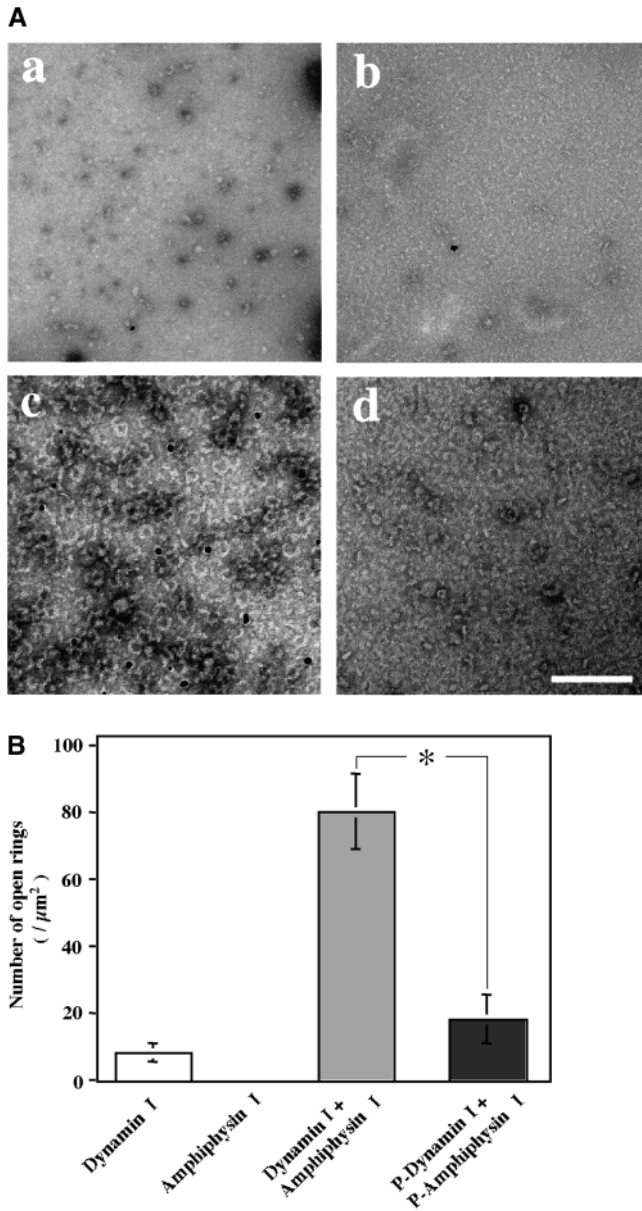
A

B

A

B

C

D

Figure 6.   **Effect of Cdk5-dependent phosphorylation of dynamin I and amphiphysin I on the ring formation.** (A) Negative staining of the proteins incubated in the absence of liposomes. (a) Dynamin-1 alone formed only a very few rings under physiological ionic strength conditions. (b) Amphiphysin I alone never formed rings. (c) A mixture of dephospho-amphiphysin I and dephospho-dynamin I produced a number of massive rings. (d) A mixture of phospho-amphiphysin I and phospho-dynamin I produced rings, but the number of rings was markedly less than that produced by a mixture of dephosphorylated forms of these proteins. Bar, 200 nm. (B) Comparison of the ring formation under each condition shown in A. The numbers of rings formed (<50 nm in diameter) from four independent experiments were averaged and graphed. Data are given as mean ($\pm$SEM). *, $P < 0.01$ (by the Scheffe's test following two-way ANOVA).

Figure 7.   **Cdk5-dependent phosphorylation of amphiphysin I and dynamin I in synaptosome and brain slices.** (A) Characterization of phosphospecific antibody for dynamin I at Thr 780. Purified dynamin I was incubated with/without recombinant Cdk5/p35 in the presence of ATP. The samples (100 ng) were subjected to SDS-PAGE, and Western blotting analysis was performed using the phosphospecific antibodies (top) and other antibodies that recognized total dynamin I (bottom). (B) Comparison of the phosphorylation of both amphiphysin I and dynamin I in the synaptosomes between wild-type and p35 knockout mice. Purified synaptosomes were incubated for 5 min in high K$^+$ buffer (High K$^+$) or were incubated with 1 μM FK506 for 5 min in control buffer as described in the Materials and methods. (C) Dynamin I undergoes electric stimulation–dependent dephosphorylation in hippocampal slices. Hippocampal slices were given electrical stimulation (10 Hz, 1 min) in the presence or absence of olomoucine, FK506, and VDCC inhibitors. Western blot analysis was performed using phosphospecific and total dynamin I antibodies. (D) Quantification of phospho-dynamin I expression from the results of C. The amount of phospho-dynamin I in each sample was normalized by each total amount of dynamin I expression, and the amount is presented as a percentage of the values measured in control slices.

lation markedly increased in the presence of FK506 (Fig. 7 B). Moreover, high K$^+$ stimulation reduced the expression of phospho-dynamin I in the synaptosomes from wild-type brain. In the synaptosomes from p35 knockout mouse brain, in contrast, the antibodies did not detect the phospho-dynamin I expression even in the presence of FK506 (Fig. 7 B).
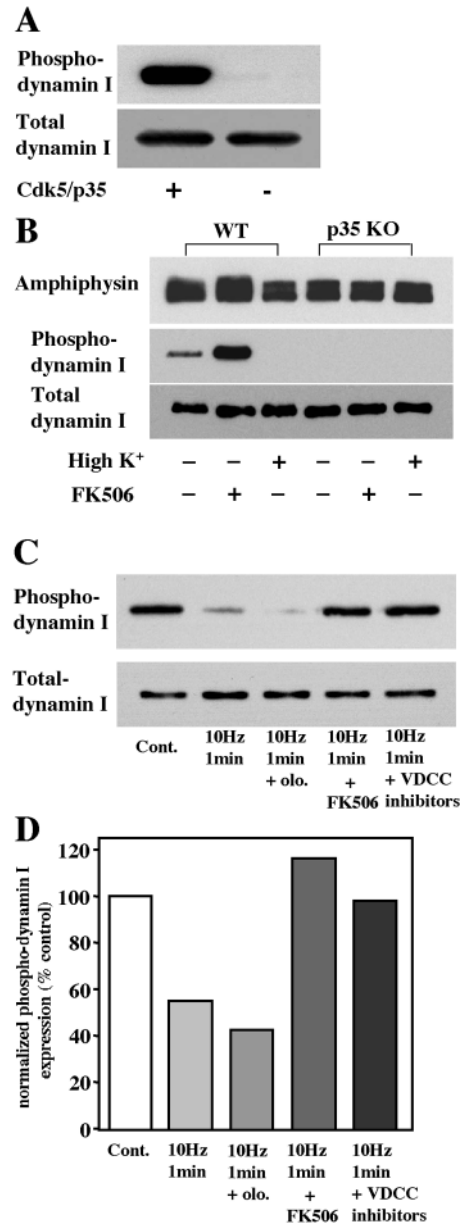
The increase in intracellular Ca^{2+} in presynaptic terminals induces calcineurin activity, resulting in the triggering of synaptic vesicle endocytosis (Cousin and Robinson, 2001). Next, whether electric stimulation (10 Hz, 1 min) changed the expression of phospho-dynamin I in hippocampal slices was examined. The stimulation reduced the level of expression of phospho-dynamin I (Fig. 7, C and D), and olomoucine enhanced the effect of electric stimulation on the reduction in the phospho-dynamin I expression level. Preincubation with FK506 (1 μM) inhibited the effect of electric stimulation on the reduction in phospho-dynamin I expression (Fig. 7, C and D). To examine whether this phenomenon occurred in presynaptic terminals, we applied specific inhibitors of N-type and P/Q-type voltage-dependent calcium channels (VDCCs) and then electrically stimulated the hippocampal slices using a protocol of 10 Hz for 1 min. N- and P/Q-type VDCCs predominantly mediate excitatory neurotransmitter release in the hippocampus (Wheeler et al., 1996). Coapplication of ω-CgTxGVIA and ω-AgaIVA, which are specific inhibitors of N-type and P/Q-type VDCCs, respectively, abrogated the effect of the electrical stimulation on the inhibition of expression level of phospho-dynamin I (Fig. 7, C and D). These results suggest that the phosphorylation of both amphiphysin I and dynamin I is regulated by Cdk5/p35 and calcineurin in the presynaptic terminals of neurons.

Discussion

Synaptic vesicle exocytosis and endocytosis are tightly regulated by changes in intracellular Ca^{2+} associated with membrane depolarization at the active zone. Synaptotagmin has been suggested to be the calcium sensor for exocytosis (Li et al., 1995; Wigge and McMahon, 1998). In contrast, calcineurin is involved in the regulation of synaptic endocytosis through the dephosphorylation of endocytic proteins (Cousin and Robinson, 2001).

Regarding the relationship between Cdk5/p35 and amphiphysin I, a previous study showed that a complex of Cdk5 and p25, a truncated form of p35, is associated with amphiphysin I in bovine brain extract (Rosales et al., 2000). Amphiphysin I interacts with p35 and is phosphorylated by Cdk5 (Floyd et al., 2001). However, it has been unclear whether Cdk5 regulates the endocytosis of synaptic vesicles through interaction with and phosphorylation of amphiphysin I. Our present results show for the first time that Cdk5-dependent phosphorylation of amphiphysin I has a critical role in the regulation of synaptic vesicle endocytosis.

Most recently, a concomitantly conducted study by Tan et al. (2003) also found that Cdk5 regulates synaptic vesicle endocytosis through the phosphorylation of dynamin I. However, their results showed that Cdk5 enhances the endocytosis similarly to calcineurin, and the phosphorylation sites they identified differ from the site we have identified here. It is hard to explain the discrepancy between these two studies. One possibility is that Tan et al. (2003) used bacterially expressed GST-Cdk5/p25 fusion protein, while the present study used the more

nearly physiological form of Cdk5/p35 derived from eukaryotic expression. This form is more than 100-fold more active than the bacterial form (unpublished data). The difference of recombinant Cdk5 and its activator may have caused the discrepancy of the identified phosphorylation sites of dynamin I by Cdk5 (Figs. 2 and 3). Another possibility is the pharmacological specificity of Cdk5 inhibitors. In the present study, we applied 10 μM roscovitine in the hippocampal neurons, as well as olomoucine, and confirmed the occurrence of consistent effects. We also showed that synaptic vesicle endocytosis was enhanced in the neurons of p35-deficient mice. Moreover, we confirmed the importance of the phosphorylation of threonine 780 of dynamin I in vesicle recycling by FM dye experiments in GFP-dynamin I mutant–overexpressing neurons (Fig. S1, available at http://www.jcb.org/cgi/content/full/jcb.200308110/DC1). Our results agree with the theory of calcineurin-dependent regulation of the clathrin-mediated endocytosis.

Seven proteins (dynamin I, amphiphysin I and II, synaptojanin, epsin, AP180, and Eps15) have been identified as targets of calcineurin (Cousin and Robinson, 2001). These proteins act at different stages of synaptic vesicle endocytosis. Epsin, AP180, and Eps15 regulate the nucleation stage of endocytosis (Cousin and Robinson, 2001). In contrast, both amphiphysin I and dynamin I mediate invagination and vesicle fission of synaptic vesicles. The question arises of whether Cdk5/p35 phosphorylates all these proteins and regulates synaptic vesicle endocytosis at all stages. In the present study, we identified the PRDs of both amphiphysin I and dynamin I as Cdk5-dependent phosphorylation sites. Cdk5 is one of the proline-directed kinases and phosphorylates the SP and TP motifs (Dhavan and Tsai, 2001). These motifs are abundant in PRD. Synaptojanin, EPS15, and amphiphysin II also have PRDs (Cousin and Robinson, 2001). Moreover, one previous study showed that cdc2 kinase phosphorylates epsin and Eps15, and the phosphorylation inhibits the interaction with AP2 (Chen et al., 1999). However, cdc2 is expressed in mitotic cells, and the expression is very low in mature neurons. Cdk5 is a member of the cdc2 kinase family, and its phosphorylation motif closely resembles that of cdc2 (Dhavan and Tsai, 2001). Therefore, Cdk5/p35 may physiologically phosphorylate epsin and Eps15 and may regulate synaptic vesicle endocytosis through the phosphorylation of all these proteins at all stages.

The mechanism of the regulation of synaptic vesicle endocytosis by phosphorylation and dephosphorylation remains controversial. Two possibilities have been proposed for the mechanism as follows: (1) regulation of protein–protein interactions and subcellular localization; and (2) regulation of the enzyme activity of dynamin I. At the fission stage, dynamin I assembles into rings around the neck of invaginated vesicles to form a collar (Hinshaw, 2000). The liposome-ring formation activity of dynamin I is enhanced by the addition of amphiphysin I (Takei et al., 1999). It has been unclear whether the effect of amphiphysin I is due to enhanced recruitment of dynamin I to the vesicle neck or stimulation of the GTPase activity of dynamin I. The present results showed that Cdk5-depen-

dent phosphorylation of amphiphysin I and dynamin I inhibited the interaction with the partner proteins. Furthermore, cophosphorylation of amphiphysin I and dynamin I completely disrupted the vesicle formation from liposomes. These data provide strong evidence that phosphorylation and dephosphorylation of endocytic proteins regulate endocytosis by altering protein–protein interactions.

In conclusion, the findings of the present study suggest that cophosphorylation of both amphiphysin I and dynamin I by Cdk5 is critical for the inhibition of synaptic vesicle endocytosis. The switching from the phosphorylated form of these proteins to the dephosphorylated form after membrane depolarization results in the reconstitution of protein–protein interaction and induction of synaptic vesicle endocytosis.

Materials and methods

Preparation of recombinant amphiphysin I, dynamin I, and Cdk5/p35 and purification of dynamin I

Full-length cDNA encoding human amphiphysin I was cloned from a human retina cDNA library (Stratagene) by PCR. After confirmation of the full sequence, the PCR products were subcloned into pGEX-6P (Amersham Biosciences). GST-tagged amphiphysin I was expressed and purified as described previously (Tomizawa et al., 2002). Finally, the GST-tagged proteins were cleaved with PreScission Protease (Amersham Biosciences) to remove GST, and amphiphysin I was purified by glutathione–Sepharose chromatography following the manufacturer's protocol (Amersham Biosciences).

Dynamin 1 was purified from bovine brain essentially as described previously (Liu et al., 1994). Human dynamin I cDNA encoding the PRD domain was subcloned into pGEX-6P, and the PRD domain mutant construct was made using QuickChange site-directed mutagenesis kit (Stratagene). Recombinant Cdk5/p35 was prepared using a baculovirus expression system as described previously (Saito et al., 2003).

In vitro phosphorylation and binding assay

The phosphorylation reaction and binding assay were performed as described previously (Tomizawa et al., 2000, 2002). In brief, phosphorylation reactions were performed in kinase buffer containing 20 mM MOPS, pH 7.4, 5 mM MgCl$_2$, 100 μM ATP, [γ-^{32}P]ATP (300 dpm/pmol), and 1 mM DTT. Purified dynamin I and amphiphysin I were incubated with each of the tested concentrations of His-tagged Cdk5/p35 at 32°C. The reactions were terminated by the addition of boiled SDS sample buffer. After electrophoresis of the samples on SDS-PAGE and staining with Coomassie blue, the relevant gel slices were excised and Cerenkov counted to determine the total ^{32}P incorporation.

For binding assays for dynamin I and amphiphysin I, dynamin I or amphiphysin I was phosphorylated by Cdk5/p35 in kinase buffer without [γ-^{32}P]ATP for 1 h at 32°C. To remove His-tagged Cdk5/p35 complex and ATP, the phospho-dynamin I and -amphiphysin I were incubated with ProBond nickel-chelating resin (Invitrogen) in PBS with 0.5% Triton X-100 for 1 h at 4°C. After centrifugation, the supernatants were dialyzed against PBS overnight at 4°C (phospho-dynamin I or -amphiphysin I). Either phospho- (5 μg) or dephospho-amphiphysin I (5 μg) was incubated with phospho- (4 μg) or dephospho-dynamin I (4 μg) in RIPA buffer (150 mM NaCl, 50 mM Tris-HCl, pH 7.5, 0.4% NP-40) for 30 min at 4°C, and 1 μg of anti–dynamin I polyclonal antibody (C-16; Santa Cruz Biotechnology), anti–amphiphysin I monoclonal antibody (Transduction Laboratories), mouse IgG, or rabbit IgG was then added for 1 h at 4°C. After the addition of 40 μl of protein G–Sepharose (Amersham Biosciences), the complex was further incubated for 1 h at 4°C. The beads were washed three times with RIPA buffer, and bound proteins were analyzed by Western blotting analysis. For the binding assay of amphiphysin I to clathrin, phospho- or dephospho-amphiphysin I was incubated with 1 mg of adult rat brain lysate in RIPA buffer with protease and phosphatase inhibitors for 1 h at 4°C. Amphiphysin I complexes were then immunoprecipitated with 1 μg of anti–amphiphysin I antibody as described above, and β-adaptin binding was then analyzed using anti–β-adaptin antibody (Transduction Laboratories). The quantification of binding proteins was performed by scanning x-ray films and analyzing the scanned images with the NIH image program.

Mass spectrometry

Sample solution (0.5 μl) was loaded onto a MALDI-MS sample plate with 0.5 μl of matrix solution (60 g/liter) of 2,5-dihydroxybenzoic acid in ACN/water (1/2, vol/vol) containing 0.1% TFA. The sample–matrix solution was allowed to air dry at room temperature. MALDI-MS measurements were obtained using a PerSeptive Voyager Linear DE model (Applied Biosystems). The remaining 90% (4.5 μl) of samples were analyzed by means of electrospray ionization (ESI) MS combined with HPLC. HPLC separations were made with a C18 silica gel column (Magicms C18 50 mm × 0.1 mm, 200 Å, 5 μm; Michrom BioResources, Inc.) at a flow-rate of ∼1 μl/min. The eluent from the HPLC column was connected directly to the ESI source. Mobile phase A was ACN/aqueous 0.2% acetic acid (5:95, vol/vol), and mobile phase B was ACN/ aqueous 0.2% acetic acid (95:5). A linear gradient program was run from 0 to 50% B over a period of 60 min. LC-MS and LC-MS/MS analyses were performed with an ESI ion trap mass spectrometer (LCQ; ThermoFinnigan) operated in a mode that alternated single MS scans (m/z 600–2000) with MS/MS scans (data-dependent scan mode in which the most intense ion peak in the previous MS scan was isolated and subjected to collision-induced dissociation).

In vitro small vesicle formation

Large unilamellar liposomes composed of 80% (wt/wt) brain extract and 20% cholesterol (1 mg/ml) were prepared as described previously (Takei et al., 2001). The liposomes (final concentration 100 μg/ml) were incubated in 1 ml of "cytosolic buffer" (25 mM Hepes-KOH, pH 7.2, 25 mM KCl, 2.5 mM magnesium acetate, 100 mM potassium glutamate) for 15 min at 37°C with proteins and GTP at the various combinations indicated. The final concentrations of proteins and nucleotides were as follows: phosphorylated or dephosphorylated dynamin, 1 or 20 μg/ml; phosphorylated or dephosphorylated amphiphysin, 1 or 50 μg/ml; GTP, 1 mM.

DLS assay

The sizes of the lipid vesicles and relative distribution in numbers of each size of lipid vesicle were measured by DLS using a DLS-7000 AR-III spectrophotometer (Otsuka Electronics Co.) as described previously (Kinuta et al., 2002).

EM

For negative staining, samples were adsorbed onto freshly glow-discharged Formvar- and carbon-coated EM grids, stained with 2% uranyl acetate in ddH$_2$O for 1 min, blotted, and air dried. The grids were examined using a Hitachi H-7100 transmission EM (Hitachi Ltd.) at the Central Research Laboratory at Okayama University Medical School.

Hippocampal neuronal culture and FM1-43 experimental conditions

Dissociated neuronal culture was performed using a modification of a previously described procedure (Matsushita et al., 2001). p35 mutant hippocampal neuronal cultures were prepared from E17–18 of hetero p35 mutant mice (Ohshima et al., 2001). The hippocampal cells from each embryo were plated onto the coated glass-bottom dishes separately. The genotype of neuronal cultures was identified from each mouse embryo.

Cultures at day 9–14 after plating were used in fluorescence experiments. The culture was superfused with normal saline solution at room temperature. The normal saline solution contained 119 mM NaCl, 2.5 mM KCl, 2 mM CaCl$_2$, 2 mM MgCl$_2$, 25 mM Hepes (pH 7.4), and 20 mM glucose. To load FM1-43 dye into the vesicles, field stimulation at 20 Hz, 30 s, duration 1.0 ms, and intensity 15 V was delivered to the culture through a parallel platinum–iridium electrode immersed into the perfusion chamber. Kynurenic acid (5 mM; Sigma-Aldrich) and D-2-amino-5-phosphonopentanoic acid (25 μM; Sigma-Aldrich) were applied during loading and unloading stimulation to prevent recurrent activity. FM1-43 dye (15 μM; Molecular Probes) was present in the superfusing solution from 45 s before stimulation to 45 s after stimulation. After FM1-43 loading, the culture was rinsed with dye-free superfusing solution for 10 min, and fluorescence imaging was performed. An unloading stimulation (10 Hz, 45 s or 20 Hz, 30 s) was delivered to the culture in the dye-free solution to unload the previously loaded dye. To label the total recycling vesicle pools, FM1-43 was loaded and unloaded by depolarization with 90 mM KCl solution. To measure the kinetics of vesicle endocytosis, FM1-43 was loaded after a delay time after the cessation of depolarization.

Fluorescence imaging and data analysis

Optical imaging experiments were performed with a Carl Zeiss MicroImaging, Inc. Axiovert 200 inverted microscope. FM1-43 fluorescence was

excited at 488 nm with a Xenon lamp. The illumination and exposure to the CCD camera (Hamamatsu Photonics) were controlled and synchronized using AquaCosmos software to minimize photobleaching of the dye. A Carl Zeiss MicroImaging, Inc. 63x/1.4 NA (Plan Apochromat) was used to view the cells, and a narrow bandpass FITC filter was used when capturing the fluorescence images.

The active boutons were measured by subtracting the unloading image from the loading image. The resulting image was filtered by thresholding at a level of mean plus four standard deviations of the Gaussian background intensity. The remaining puncta were taken as activity-dependent boutons. These boutons showed uptake of the FM1-43 dye during vesicle recycling, thus reflecting endocytosis.

Production of phosphospecific antibodies for dynamin I and immunoblot analysis
A peptide corresponding to residues 772–784 of rat dynamin I was chemically phosphorylated at residue Thr 780 and employed to generate rabbit polyclonal antibodies that specifically detected phospho-dynamin I as described previously (Czernik et al., 1991). Western blot analysis was performed at high stringency, essentially as described previously (Tomizawa et al., 2002).

Generation of p35 knockout mice and preparation of synaptosomes
p35 mutant mice were generated and maintained in a 129/Sv × C57BL/6J background as described previously (Ohshima et al., 2001). Synaptosomes were prepared from wild-type and p35 knockout mice as described previously (Tomizawa et al., 2002). Stimulation (depolarization) of synaptosomes was performed as described previously (Bauerfeind et al., 1997). FK506 (1 μM) was incubated with synaptosomes for 5 min in control buffer. Incubations were terminated by adding SDS-PAGE buffer, and the samples were used for Western blotting analysis.

Preparation of hippocampal slices and electric stimulation
Preparation of hippocampal slices and electric stimulation were performed as described previously (Tomizawa et al., 2002). In brief, the hippocampus of male C57BL/6 mice aged 7–8 wk was dissected, and 400-μm transverse slices were prepared. A bipolar stimulating electrode was placed along the Schaffer collateral fibers, and a glass micropipette filled with artificial cerebrospinal fluid was placed in the stratum radiatum of the CA1 region to record field excitatory postsynaptic potentials (EPSPs) and to adjust the intensity of the stimulation. The intensity of the stimulation was adjusted to produce an EPSP with a slope of 50% of the maximum.

ω-Conotoxin GVIA (ω-CgTX GVIA; RBI), ω-Agatoxin IVA (ω-Aga IVA; RBI), and FK506 (Fujisawa Pharmaceutical) were added to the perfusion medium. The final concentration of ω-CgTX GVIA and FK506 was 1 μM, and the final concentration of ω-Aga IVA was 0.5 μM. After preincubation with these drugs for 30 min, hippocampal slices were electrically stimulated with 10 Hz for 1 min, and the slices were then sonicated in boiled 1% SDS.

Statistical analysis
Data were analyzed using either the t test to compare the two conditions or ANOVA followed by planned comparisons of the multiple conditions, and $P < 0.05$ was considered to be significant.

Online supplemental material
The supplemental material (Fig. S1) is available online at http://www.jcb.org/cgi/content/full/jcb.200308110/DC1. Fig. S1 shows enhancement of vesicle endocytosis in hippocampal neurons overexpressing dynamin I mutant at Thr 780.

References

Bauerfeind, R., K. Takei, and P. De Camilli. 1997. Amphiphysin I is associated with coated endocytic intermediates and undergoes stimulation-dependent dephosphorylation in nerve terminals. *J. Biol. Chem.* 272:30984–30992.

Bibb, J.A., J. Chen, J.R. Taylor, P. Svenningsson, A. Nishi, Z. Yan, Z.K. Sagawa, A.C. Nairn, E.J. Nestler, and P. Greengard. 2001. Effects of chronic exposure to cocaine are regulated by the neuronal protein Cdk5. *Nature.* 410:376–380.

Brodin, L., P. Low, and O. Shupliakov. 2000. Sequential steps in clathrin-mediated synaptic vesicle endocytosis. *Curr. Opin. Neurobiol.* 10:312–320.

Chen, H., V.I. Slepnev, P.P. Di Fiore, and P. De Camilli. 1999. The interaction of epsin and Eps15 with the clathrin adaptor AP-2 is inhibited by mitotic phosphorylation and enhanced by stimulation-dependent dephosphorylation in nerve terminals. *J. Biol. Chem.* 274:3257–3260.

Cousin, M.A., and P.J. Robinson. 2001. The dephosphins: dephosphorylation by calcineurin triggers synaptic vesicle endocytosis. *Trends Neurosci.* 24:659–665.

Cremona, O., and P. De Camilli. 1997. Synaptic vesicle endocytosis. *Curr. Opin. Neurobiol.* 7:323–330.

Czernik, A.J., J.-A. Girault, A.C. Nairn, J. Chen, G. Snyder, J. Kebabian, and P. Greengard. 1991. Production of phosphorylation state-specific antibodies. *In* Methods in Enzymology. T. Hunter and B.M. Sefton, editors. Academic Press Inc., New York. 264–283.

David, C., P.S. McPherson, O. Mundigl, and P. De Camilli. 1996. A role of amphiphysin in synaptic vesicle endocytosis suggested by its binding to dynamin in nerve terminals. *Proc. Natl. Acad. Sci. USA.* 93:331–335.

Dhavan, R., and L.-H. Tsai. 2001. A decade of Cdk5. *Nat. Rev. Mol. Cell Biol.* 2:749–759.

Di Paolo, G., S. Sankaranarayanan, M.R. Wenk, L. Daniell, E. Perucco, B.J. Caldarone, R. Flavell, M.R. Picciotto, T.A. Ryan, O. Cremona, and P. De Camilli. 2002. Decreased synaptic vesicle recycling efficiency and cognitive deficits in amphiphysin 1 knockout mice. *Neuron.* 33:789–804.

Floyd, S.R., E.B. Porro, V.I. Slepnev, G.C. Ochoa, L.-H. Tsai, and P. De Camilli. 2001. Amphiphysin 1 binds the cyclin-dependent kinase (cdk) 5 regulatory subunit p35 and is phosphorylated by cdk5 and cdc2. *J. Biol. Chem.* 276:8104–8110.

Hinshaw, J.E. 2000. Dynamin and its role in membrane fission. *Annu. Rev. Cell Dev. Biol.* 16:483–519.

Kinuta, M., H. Yamada, T. Abe, M. Watanabe, S.-A. Li, A. Kamitani, T. Matsukawa, T. Yasuda, H. Kumon, and K. Takei. 2002. Phosphatidylinositol 4,5-bisphosphate stimulates vesicle formation from liposomes by brain cytosol. *Proc. Natl. Acad. Sci. USA.* 99:2842–2847.

Li, C., B. Ullrich, J.Z. Zhang, R.G. Anderson, N. Brose, and T.C. Südhof. 1995. Ca^{2+}-dependent and -independent activities of neural and non-neural synaptotagmins. *Nature.* 375:594–599.

Liu, J.P., K.A. Powell, T.C. Südhof, and P.J. Robinson. 1994. Dynamin I is a Ca^{2+}-sensitive phospholipid-binding protein with very high affinity for protein kinase C. *J. Biol. Chem.* 269:21043–21050.

Marks, B., and H.T. McMahon. 1998. Calcium triggers calcineurin-dependent synaptic vesicle recycling in mammalian nerve terminals. *Curr. Biol.* 8:740–749.

McMahon, H.T., P. Wigge, and C.C. Smith. 1997. Clathrin interacts specifically with amphiphysin and is displaced by dynamin. *FEBS Lett.* 413:319–322.

Matsubara, M., M. Kusubata, K. Ishiguro, T. Uchida, K. Titani, and H. Taniguchi. 1996. Site-specific phosphorylation of synapsin I by mitogen-activated protein kinase and Cdk5 and its effects on physiological functions. *J. Biol. Chem.* 271:21108–21113.

Matsushita, M., K. Tomizawa, A. Moriwaki, S.-T. Li, H. Terada, and H. Matsui. 2001. A high-efficiency protein transduction system demonstrating the role of PKA in long-lasting long-term potentiation. *J. Neurosci.* 21:6000–6007.

Ohshima, T., M. Ogawa, Veeranna, M. Hirasawa, G. Longenecker, K. Ishiguro, H.C. Pant, R.O. Brady, A.B. Kulkarni, and K. Mikoshiba. 2001. Synergistic contribution of Cdk5/p35 and Reelin/Dab1 to the positioning of cortical neurons in the developing mouse brain. *Proc. Natl. Acad. Sci. USA.* 98:2764–2769.

Owen, D.J., P. Wigge, Y. Vallis, J.D.A. Moore, P.R. Evans, and H.T. McMahon. 1998. Crystal structure of the amphiphysin-2 SH3 domain and its role in the prevention of dynamin ring formation. *EMBO J.* 17:5273–5285.

Pyle, J.L., E.T. Kavalali, E.S. Piedras-Renteria, and R.W. Tsien. 2000. Rapid reuse of readily releasable pool vesicles at hippocampal synapses. *Neuron.* 28:221–231.

Rosales, J.L., M.J. Nodwell, R.N. Johnston, and K.-Y. Lee. 2000. Cdk5/p25[nck5a] interaction with synaptic proteins in bovine brain. *J. Cell. Biochem.* 78:151–159.

Saito, T., R. Onuki, Y. Fujita, G. Kusakawa, K. Ishiguro, J.A. Bibb, T. Kishimoto, and S. Hisanaga. 2003. Developmental regulation of the proteolysis of the

p35, Cdk5 activator, by phosphorylation. *J. Neurosci.* 23:1189–1197.

Shuang, R., L. Zhang, A. Fletcher, G.E. Groblewski, J. Pevsner, and E.L. Stuenkel. 1998. Regulation of Munc-18/syntaxin 1A interaction by cyclin-dependent kinase 5 in nerve endings. *J. Biol. Chem.* 273:4957–4966.

Slepnev, V.I., G.-C. Ochoa, M.H. Butler, D.G. Grabs, and P. De Camilli. 1998. Role of phosphorylation in regulation of the assembly of endocytic coat complexes. *Science.* 281:821–824.

Takei, K., and V. Haucke. 2001. Clathrin-mediated endocytosis: membrane factors pull the trigger. *Trends Cell Biol.* 11:385–391.

Takei, K., V.I. Slepnev, V. Haucke, and P. De Camilli. 1999. Functional partnership between amphiphysin and dynamin in clathrin-mediated endocytosis. *Nat. Cell Biol.* 1:33–39.

Takei, K., V.I. Slepnev, and P. De Camilli. 2001. Interactions of dynamin and amphiphysin with liposomes. *Methods Enzymol.* 329:478–486.

Tan, T.C., V.A. Valova, C.S. Malladi, M.E. Graham, L.A. Berven, O.J. Jupp, G. Hansra, S.J. McClure, B. Sarcevic, R.A. Boadle, et al. 2003. Cdk5 is essential for synaptic vesicle endocytosis. *Nat. Cell Biol.* 5:701–710.

Tomizawa, K., X.-H. Cai, A. Moriwaki, M. Matsushita, and H. Matsui. 2000. Involvement of cyclin-dependent kinase 5/p35[nck5a] in the synaptic reorganization of rat hippocampus during kindling progression. *Jpn. J. Physiol.* 50: 525–532.

Tomizawa, K., J. Ohta, M. Matsushita, A. Moriwaki, S.-T. Li, K. Takei, and H. Matsui. 2002. Cdk5/p35 regulates neurotransmitter release through phosphorylation and downregulation of P/Q-type voltage-dependent calcium channel activity. *J. Neurosci.* 22:2590–2597.

Vesely, J., L. Havlicek, M. Strnad, J.J. Blow, A. Donella-Deana, L. Pinna, D.S. Letham, J. Kato, L. Détivaud, S. Leclerc, and L. Meijer. 1994. Inhibition of cyclin-dependent kinases by purine analogues. *Eur. J. Biochem.* 224:771–786.

Wang, L.H., T.C. Südhof, and R.G.W. Anderson. 1995. The appendage domain of alpha-adaptin is a high affinity binding site for dynamin. *J. Biol. Chem.* 270:10079–10083.

Wheeler, D.B., A. Randall, and R.W. Tsien. 1996. Change in action potential duration alters reliance of excitatory synaptic transmission on multiple types of Ca^{2+} channels in rat hippocampus. *J. Neurosci.* 16:2226–2237.

Wigge, P., and H.T. McMahon. 1998. The amphiphysin family of proteins and their role in endocytosis at the synapse. *Trends Neurosci.* 21:339–344.